Optimal Sharing of Public Transport Lanes

Mehdi Naderi*[1], Milad Malekzadeh[2], and Zdeněk Hurák[3]

[1]Postdoctoral researcher, Faculty of Electrical Engineering, Czech Technical University in Prague, Czechia
[2]Postdoctoral researcher, TUM School of Engineering and Design, Technical University of Munich, Germany
[3]Faculty of Electrical Engineering, Czech Technical University in Prague, Czechia

Short summary

Urban traffic congestion represents a significant contemporary challenge, attracting considerable research interest in its mitigation. In light of the inherent difficulty and expense involved in infrastructure expansion, enhancing the exploitation level of existing infrastructure is deemed highly advantageous. This paper proposes a strategy to share the lanes dedicated to public transport fleets, e.g. buses or trams, with the passenger cars to improve the traffic condition. Employing the Cell Transmission Model (CTM), an Optimal Control Problem (OCP) is formulated to determine the lateral flow between the main road and the dedicated lane without any disruption to the public transport schedule. The OCP cost function is defined to minimize total travel time and unnecessary lateral movement, while CTM equations and the public fleet timetable are implemented as the OCP constraints. The preliminary findings from macroscopic simulation experiments indicate that the proposed approach enhances traffic conditions.
Keywords: Lateral flow control, lane sharing, optimal control.

1 Introduction

The advancement of urban mobility, despite its advantages, has precipitated considerable traffic congestion, particularly within urban areas, causing long delays, increased air pollution, and safety degradation. Infrastructure expansion represents a possible strategy for enhancing traffic management; however, its significant cost, prolonged duration, and adverse ecological impact are notable drawbacks (Keyvan-Ekbatani et al. (2012)). Enhancing the exploitation level of established infrastructure is a sensible alternative that has been the focus of considerable academic and industry research.

A method of improving highway utilization is *tidal flow control*, a lane management strategy that allocates an appropriate number of lanes to each traffic direction (Ampountolas et al. (2019)). The lane configuration may be established through static methodologies, which utilize historical data and assign lane direction based on space and time, or dynamic approaches, which incorporate real-time measurements. Additionally, *Internal Boundary Control (IBC)*, proposed by Malekzadeh et al. (2021), is a tidal control strategy, applicable in lane-free highways at a high penetration rate of Connected Automated Vehicles (CAVs). For a comprehensive review of tidal flow control approaches, the reader is referred to Malekzadeh et al. (2025). Some studies, such as those by Ampountolas et al. (2019); Li et al. (2023), in particular, have investigated the implementation of a reversible buffer lane situated in the road's median, with the capacity to alter its direction to alleviate traffic congestion.

In urban traffic, the dedicated space to public transport can serve as irreversible buffer lane. Specifically, a portion of traffic can be rerouted to utilize the dedicated lanes when doing so does not impede the public transport timetable. A discussed proposal in light of CAVs involves co-sharing public transport lanes, aiming to optimize infrastructure usage and alleviate challenges posed by mixed traffic conditions (Zhang et al. (2025)). Empirical investigations have substantiated that a dedicated lane for CAVs and buses enhances their travel performance and concurrently diminishes overall expenses Luo et al. (2022). Also, Shan et al. (2024) proposed a dynamic bus lane management approach that incorporates joint path planning of CAVs and automated buses, resulting in significant improvement in time delay and fuel consumption. Furthermore, Liang et al. (2026) focused on lane changing phase of CAVs that can use the bus dedicated lanes, while

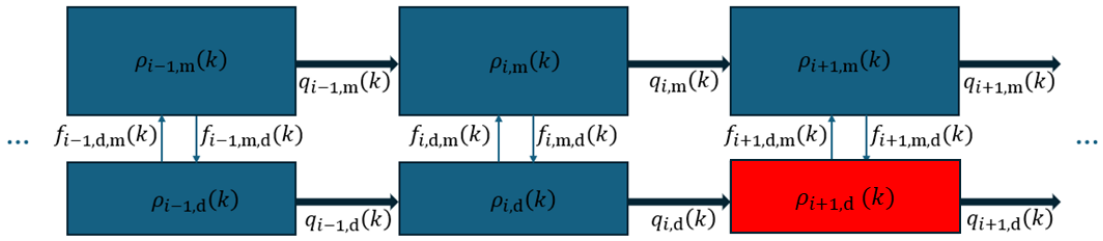


Figure 1: Road sketch

preserving buses priority. Such studies illustrate that shared lanes among public transport and CAVs could lead to improved traffic conditions; however, the dedicated lanes cannot handle all CAVs when the market penetration rate is high Jiang & Shang (2022).
To the best of our knowledge, literature lacks a comprehensive macroscopic study of sharing dedicated lanes with passenger cars, which, at least theoretically, could be either human-driven or automated. This paper initially establishes a macroscopic model to simulate traffic rerouting to and from the dedicated lanes. Thereafter, the lateral flows are determined by solving an optimal control problem (OCP). Specifically, the optimal lateral flow defines the volume, timing, and location of traffic directed to the dedicated lanes. It also specifies when and where vehicles should exit the dedicated lanes in order to avoid disrupting the public transport schedule. Macroscopic modeling and simulation present an opportunity for traffic management authorities and policymakers to comprehend the potential improvements in traffic conditions resulting from dedicated lane-sharing.

2 Macroscopic Model

The design of traffic control systems is often approached from a macroscopic perspective, utilizing aggregated variables with parameters identifiable through empirical data. The macroscopic controller demonstrates applicability to both human-operated and autonomous vehicles, aligning effectively with our objective. The dynamics of traffic and the application of dedicated lanes are modeled within this paper through a CTM model, which is established based on the framework from Roncoli et al. (2015a,b) that uses the triangular fundamental diagram. Consider a road including dedicated space for public transport whose variables are defined below (see Fig. 1):

- $q_{i,\mathrm{m}}(k)$: The mainstream flow from cell $i-1$ to cell i in the interval of $[kT,(k+1)T]$ on the main road
- $q_{i,\mathrm{d}}(k)$: The mainstream flow from cell $i-1$ to cell i in the interval of $[kT,(k+1)T]$ on the dedicated lane
- $\rho_{i,\mathrm{m}}(k)$: The density at cell i at kT on the main road
- $\rho_{i,\mathrm{d}}(k)$: The density at cell i at kT on the dedicated lane
- $f_{i,\mathrm{m,d}}(k)$: The flow entering cell i of the dedicated lane from the main road in the interval of $[kT,(k+1)T]$
- $f_{i,\mathrm{d,m}}(k)$: The flow leaving cell i of the dedicated lane to the main road in the interval of $[kT,(k+1)T]$

Note that the flow and density variables for the dedicated lane account only for passenger cars and exclude public transport vehicles. Given the introduced variables, the conservation equations can be written for the main road and the dedicated lane as below

$$\begin{aligned}\rho_{i,\mathrm{m}}(k+1) &= \rho_{i,\mathrm{m}}(k)+\frac{T}{L}\left(q_{i-1,\mathrm{m}}(k)-q_{i,\mathrm{m}}(k)+f_{i,\mathrm{d,m}}(k)-f_{i,\mathrm{m,d}}(k)\right),\\ \rho_{i,\mathrm{d}}(k+1) &= \rho_{i,\mathrm{d}}(k)+\frac{T}{L}\left(q_{i-1,\mathrm{d}}(k)-q_{i,\mathrm{d}}(k)+f_{i,\mathrm{m,d}}(k)-f_{i,\mathrm{d,m}}(k)\right)\end{aligned} \tag{1}$$

where L is the length of each cell and T is the sampling period. As the presence of a public vehicle changes the condition in a cell, L should be chosen smaller than the one for normal applications. The maximum length of bus/tram stations could be a good choice. In addition, to ensure numerical stability, the sampling period should satisfy $T \leq L/v^{\mathrm{f}}$ with v^{f} being the free-flow speed. In CTM,

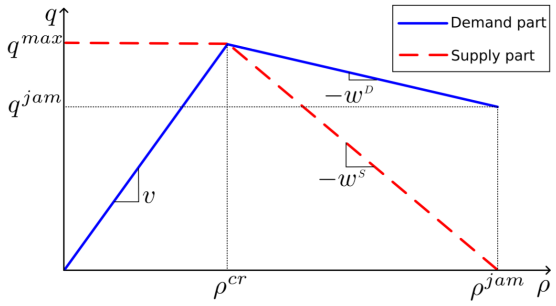


Figure 2: Supply and demand functions (Roncoli et al. (2015b))

the flow is calculated as the minimum between the downstream *demand* flow and the upstream *supply* flow. To capture the *capacity drop* phenomenon, the supply and demand functions shown in Fig. 2 are employed, which can be written as follows

$$\begin{aligned}
Q^{\mathrm{D}}_{i,\mathrm{m}}(k) &= \min\left(v^{\mathrm{f}}\rho_{i,\mathrm{m}}(k),\ -w^{\mathrm{D}}_{\mathrm{m}}\rho_{i,\mathrm{m}}(k) + g^{\mathrm{D}}_{\mathrm{m}}\right),\\
Q^{\mathrm{S}}_{i,\mathrm{m}}(k) &= \min\left(v^{\mathrm{f}}\rho^{\mathrm{cr}}_{i+1,\mathrm{m}},\ -w^{\mathrm{S}}_{\mathrm{m}}\rho_{i+1,\mathrm{m}}(k) + -g^{\mathrm{S}}_{\mathrm{m}}\right),\\
Q^{\mathrm{D}}_{i,\mathrm{d}}(k) &= \min\left(v^{\mathrm{f}}_{i,\mathrm{d}}(k)\rho_{i,\mathrm{d}}(k),\ -w^{\mathrm{D}}_{\mathrm{d}}\rho_{i,\mathrm{d}}(k) + g^{\mathrm{D}}_{\mathrm{d}}\right),\\
Q^{\mathrm{S}}_{i,\mathrm{d}}(k) &= \min\left(v^{\mathrm{f}}_{i+1,\mathrm{d}}(k)\rho^{\mathrm{cr}}_{i+1,\mathrm{d}}(k),\ -w^{\mathrm{S}}_{\mathrm{d}}\rho_{i+1,\mathrm{d}}(k) + g^{\mathrm{S}}_{\mathrm{d}}\right),
\end{aligned} \tag{2}$$

where

$$\begin{aligned}
w^{\mathrm{D}}_{\mathrm{m}} &= \frac{v^{\mathrm{f}}\rho^{\mathrm{cr}}_{i,\mathrm{m}} - q^{\mathrm{jam}}_{i,\mathrm{m}}}{\rho^{\mathrm{jam}}_{i,\mathrm{m}} - \rho^{\mathrm{cr}}_{i,\mathrm{m}}}, \quad g^{\mathrm{D}}_{\mathrm{m}} = \frac{\rho^{\mathrm{cr}}_{i,\mathrm{m}}\left(v^{\mathrm{f}}\rho^{\mathrm{jam}}_{i,\mathrm{m}} - q^{\mathrm{jam}}_{i,\mathrm{m}}\right)}{\rho^{\mathrm{jam}}_{i,\mathrm{m}} - \rho^{\mathrm{cr}}_{i,\mathrm{m}}},\\
w^{\mathrm{S}}_{\mathrm{m}} &= \frac{v^{\mathrm{f}}\rho^{\mathrm{cr}}_{i+1,\mathrm{m}}}{\rho^{\mathrm{jam}}_{i+1,\mathrm{m}} - \rho^{\mathrm{cr}}_{i+1,\mathrm{m}}}, \quad g^{\mathrm{S}}_{\mathrm{m}} = \frac{v^{f}\rho^{\mathrm{cr}}_{i+1,\mathrm{m}}\rho^{\mathrm{jam}}_{i+1,\mathrm{m}}}{\rho^{\mathrm{jam}}_{i+1,\mathrm{m}} - \rho^{\mathrm{cr}}_{i+1,\mathrm{m}}},\\
w^{\mathrm{D}}_{\mathrm{d}} &= \frac{v^{\mathrm{f}}_{i,\mathrm{d}}(k)\rho^{\mathrm{cr}}_{i,\mathrm{d}}(k) - q^{\mathrm{jam}}_{i,\mathrm{d}}}{\rho^{\mathrm{jam}}_{i,\mathrm{d}} - \rho^{\mathrm{cr}}_{i,\mathrm{d}}(k)}, \quad g^{\mathrm{D}}_{\mathrm{d}} = \frac{\rho^{\mathrm{cr}}_{i,\mathrm{d}}(k)\left(v^{\mathrm{f}}_{i,\mathrm{d}}(k)\rho^{\mathrm{jam}}_{i,\mathrm{d}} - q^{\mathrm{jam}}_{i,\mathrm{d}}\right)}{\rho^{\mathrm{jam}}_{i,\mathrm{d}} - \rho^{\mathrm{cr}}_{i,\mathrm{d}}(k)},\\
w^{\mathrm{S}}_{\mathrm{d}} &= \frac{v^{\mathrm{f}}_{i+1,\mathrm{d}}(k)\rho^{\mathrm{cr}}_{i+1,\mathrm{d}}(k)}{\rho^{\mathrm{jam}}_{i+1,\mathrm{d}} - \rho^{\mathrm{cr}}_{i+1,\mathrm{d}}(k)}, \quad g^{\mathrm{S}}_{\mathrm{d}} = \frac{v^{\mathrm{f}}_{i+1,\mathrm{d}}(k)\rho^{\mathrm{cr}}_{i+1,\mathrm{d}}(k)\rho^{\mathrm{jam}}_{i+1,\mathrm{d}}}{\rho^{\mathrm{jam}}_{i+1,\mathrm{d}} - \rho^{\mathrm{cr}}_{i+1,\mathrm{d}}(k)},
\end{aligned} \tag{3}$$

where v^{f} denotes the constant free-flow speed on the main road. In contrast, $v^{\mathrm{f}}_{i,\mathrm{d}}(k)$ represents the free-flow speed in the dedicated lane, which varies depending on the traffic situation. Specifically, if cell i contains a bus or tram stop and a public transport vehicle is dwelling, then $v^{\mathrm{f}}_{i,\mathrm{d}}(k) = 0$. If the cell contains a moving public transport vehicle, then $v^{\mathrm{f}}_{i,\mathrm{d}}(k)$ is set to the maximum speed of public transport fleets, denoted by v^{P}. Otherwise, $v^{\mathrm{f}}_{i,\mathrm{d}}(k)$ is set equal to the main road free-flow speed v^{f}. Given a fixed timetable and real-time information on the locations of public transport vehicles, $v^{\mathrm{f}}_{i,\mathrm{d}}(k)$ can be determined for all cells over the considered time horizon.

$$v^{\mathrm{f}}_{i,\mathrm{d}}(k) = \begin{cases} 0, & \text{if a public vehicle is stopped at a station cell,}\\ v^{\mathrm{P}}, & \text{if a public vehicle is moving in the cell,}\\ v^{\mathrm{f}}, & \text{otherwise.}\end{cases} \tag{4}$$

Moreover, $\rho^{\mathrm{cr}}_{i,\mathrm{m}}$ and $\rho^{\mathrm{cr}}_{i,\mathrm{d}}(k) = q^{\max}_{\mathrm{d}}/v^{\mathrm{f}}_{i,\mathrm{d}}(k)$ denote the critical densities of the main road and the dedicated lane, respectively, where $q^{\max}_{\mathrm{d}}$ represents the capacity of the dedicated lane for passenger cars. Note that when $v^{\mathrm{f}}_{i,\mathrm{d}}(k) = 0$, the corresponding demand or supply function becomes zero, as the first term of the minimum operator is zero; therefore, $\rho^{\mathrm{cr}}_{i,\mathrm{d}}(k)$ does not need to be computed. Furthermore, ρ^{jam} and q^{jam} denote the jam density and the corresponding flow in congested (jammed) conditions, respectively.
Since the control inputs of the proposed model are lateral flows, their values must be included in

the calculation of demand and supply, as below

$$\begin{aligned}
\hat{Q}^{\mathrm{D}}_{i,\mathrm{m}}(k) &= \min\left(Q^{\mathrm{D}}_{i,\mathrm{m}}(k),\ \frac{L}{T}\rho_{i,\mathrm{m}}(k) + f_{i,\mathrm{d,m}}(k) - f_{i,\mathrm{m,d}}(k)\right),\\
\hat{Q}^{S}_{i,\mathrm{m}}(k) &= Q^{\mathrm{S}}_{i,\mathrm{m}}(k) + f_{i+1,\mathrm{m,d}}(k) - f_{i+1,\mathrm{d,m}}(k),\\
\hat{Q}^{\mathrm{D}}_{i,\mathrm{d}}(k) &= \min\left(Q^{\mathrm{D}}_{i,\mathrm{d}}(k),\ \frac{L}{T}\rho_{i,\mathrm{d}}(k) + f_{i,\mathrm{m,d}}(k) - f_{i,\mathrm{d,m}}(k)\right),\\
\hat{Q}^{\mathrm{S}}_{i,\mathrm{d}}(k) &= Q^{S}_{i,\mathrm{d}}(k) + f_{i+1,\mathrm{d,m}}(k) - f_{i+1,\mathrm{m,d}}(k).
\end{aligned} \tag{5}$$

Finally, the longitudinal flow can be obtained by

$$\begin{aligned}
q_{i,\mathrm{m}}(k) &= \min\left(\hat{Q}^{\mathrm{D}}_{i,\mathrm{m}}(k),\ \hat{Q}^{\mathrm{S}}_{i,\mathrm{m}}(k)\right),\\
q_{i,\mathrm{d}}(k) &= \min\left(\hat{Q}^{\mathrm{D}}_{i,\mathrm{d}}(k),\ \hat{Q}^{\mathrm{S}}_{i,\mathrm{d}}(k)\right).
\end{aligned} \tag{6}$$

3 Optimal Control Problem

This section outlines the formulation of an OCP, the resolution of which determines the optimal lateral flows. To this end, we consider density of each cell of the main road and the dedicated lane as the state variables. Also, lateral flows of each cell are the control variables. Then, the state equations can be written as

$$\mathbf{x}(k+1) = \mathbf{f}(\mathbf{x}(k), \mathbf{u}(k)) \tag{7}$$

, where

$$\begin{aligned}
\mathbf{x}(k) &= \left[\rho_{1,\mathrm{m}}(k), \rho_{1,\mathrm{d}}(k), \rho_{2,\mathrm{m}}(k), \rho_{2,\mathrm{d}}(k), \cdots, \rho_{N,\mathrm{m}}(k), \rho_{N,\mathrm{d}}(k)\right]^T,\\
\mathbf{u}(k) &= \left[f_{1,\mathrm{m,d}}(k), f_{1,\mathrm{d,m}}(k), f_{2,\mathrm{m,d}}(k), f_{2,\mathrm{d,m}}(k), \cdots, f_{N,\mathrm{m,d}}(k), f_{N,\mathrm{d,m}}(k)\right]^T,
\end{aligned} \tag{8}$$

and $\mathbf{f}$ is obtained from (1). The OCP cost function containing multiple terms is

$$J = \sum_{i=1}^{N}\sum_{k=0}^{K-1}\left(w_1\rho^2_{i,\mathrm{m}}(k) + w_2\rho^2_{i,\mathrm{d}}(k) + w_3 f_{i,\mathrm{m,d}}(k) + w_4 f_{i,\mathrm{d,m}}(k)\right), \tag{9}$$

where N and K are the number of road cells and samples of the optimization horizon, respectively. The first two terms serve to reduce cell densities, which in turn elevates average speed, ultimately leading to minimized travel time. Employing a quadratic penalty facilitates the alleviation of congestion on the main road by rerouting a part of traffic to the dedicated lanes, where travel at free-flow speeds is achievable. In fact, when a public vehicle is stopped in a cell, there will be no flow through the cell; hence, the presence of passenger vehicles in the dedicated lanes causes high densities.

In addition to the state equations, some input constraints must be imposed to respect physical limits. First, the leaving flow cannot be more than available vehicles in the origin cell; and secondly, it should not exceed the available space in the destination cell. In order to preserve the public transport priority, we define different limits for entering and exiting flows to and from the dedicated lane. To keep the dedicated lane in free flow condition, the former should be so that to not exceed the critical density in the dedicated lane

$$0 \le f_{i,\mathrm{m,d}}(k) \le \frac{L}{T}\min\left(\rho_{i,\mathrm{m}}(k), \max(\rho^{\mathrm{cr}}_{i,\mathrm{d}}(k) - \rho_{i,\mathrm{d}}(k), 0\right). \tag{10}$$

On the other hand, the flow from dedicated lane to the main road can be as much as available space on the main road allows

$$0 \le f_{i,\mathrm{d,m}}(k) \le \frac{L}{T}\min\left(\rho_{i,\mathrm{d}}(k), (\rho^{\mathrm{jam}}_{i,\mathrm{m}} - \rho_{i,\mathrm{m}}(k)\right). \tag{11}$$

Moreover, a constant upper limit for lateral flows is considered

$$\begin{aligned}
f_{i,\mathrm{d,m}}(k) &\le f^{\max}\\
f_{i,\mathrm{m,d}}(k) &\le f^{\max}.
\end{aligned} \tag{12}$$

The OCP can be summarized as

$$\text{Minimize} \quad \sum_{i=1}^{N}\sum_{k=0}^{K-1}\Big(w_1\rho_{i,\mathrm{m}}^2(k)+w_2\rho_{i,\mathrm{d}}^2(k)+w_3 f_{i,\mathrm{m,d}}(k)+w_4 f_{i,\mathrm{d,m}}(k)\Big)$$

$$\begin{aligned}
&\text{subject to :}\\
&\rho_{i,\mathrm{m}}(k+1)=\rho_{i,\mathrm{m}}(k)+\frac{T}{L}\Big(q_{i-1,\mathrm{m}}(k)-q_{i,\mathrm{m}}(k)+f_{i,\mathrm{d,m}}(k)-f_{i,\mathrm{m,d}}(k)\Big),\\
&\rho_{i,\mathrm{d}}(k+1)=\rho_{i,\mathrm{d}}(k)+\frac{T}{L}\Big(q_{i-1,\mathrm{d}}(k)-q_{i,\mathrm{d}}(k)+f_{i,\mathrm{m,d}}(k)-f_{i,\mathrm{d,m}}(k)\Big),\\
&q_{i,\mathrm{m}}(k)=\min\Big(\hat{Q}_{i,\mathrm{m}}^{\mathrm{D}}(k),\ \hat{Q}_{i,\mathrm{m}}^{\mathrm{S}}(k)\Big),\\
&q_{i,\mathrm{d}}(k)=\min\Big(\hat{Q}_{i,\mathrm{d}}^{\mathrm{D}}(k),\ \hat{Q}_{i,\mathrm{d}}^{\mathrm{S}}(k)\Big),\\
&0\le f_{i,\mathrm{m,d}}(k)\le\frac{L}{T}\min\Big(\rho_{i,\mathrm{m}}(k),\ \max(\rho_{i,\mathrm{d}}^{\mathrm{cr}}(k)-\rho_{i,\mathrm{d}}(k),0)\Big),\\
&0\le f_{i,\mathrm{d,m}}(k)\le\frac{L}{T}\min\Big(\rho_{i,\mathrm{d}}(k),\ \rho_{i,\mathrm{m}}^{\mathrm{jam}}-\rho_{i,\mathrm{m}}(k)\Big),\\
&f_{i,\mathrm{d,m}}(k)\le f^{\max},\\
&f_{i,\mathrm{m,d}}(k)\le f^{\max}.
\end{aligned}\tag{13}$$

To solve the OCP, an efficient and fast approach, Feasible Direction Algorithm (FDA), developed by Papageorgiou et al. (2016), is employed. The FDA is an iterative algorithm that commences with a provided feasible control trajectory. Each iteration attempts to improve the control trajectories, in this work, using resilient backpropagation (RPROP). Finally, the algorithm converges to a local minimum of the cost function.

4 Results and discussion

The efficacy of the proposed strategy is investigated by performing a simulation on a 1 km road. With the road sectioned into ten cells, the length of each cell is 100 m. The free-flow speed of the main road and the dedicated lane is, respectively, 60 km/h and 40 km/h. A sampling period of 3 seconds has been chosen to achieve numerical stability for the CTM. Capacity of the main road (dedicated lane) is 4000 veh/h (1800 veh/h), hence the critical density is 66.7 veh/km (50 veh/km). Jam density of the main road is also 150 veh/km. The time horizon of the OCP is 300 seconds, i.e., $K = 100$. It is assumed that a public transportation stop is located within the ninth section, and the schedule specifies a stop between samples 60 and 80.

The upstream demand of the main road is shown in Fig. 3 which exceeds the capacity of the main road during a specific period, leading to the formation of a queue, as can be observed in (Fig. 4). When no sharing strategy is implemented, passenger vehicles merely traverse the main road. Once critical density is achieved, extra vehicles are kept in queues, consequently increasing their travel times. Figure 5 shows the density of the road sections in this condition, showing that the density of the main road persists at the critical density for an extended period when the demand upstream exceeds the capacity to handle the vehicles in the queue.

Alternatively, the adoption of the sharing strategy results in the alleviation of the upstream queue and a decrease in the duration of the interval wherein the main road experiences critical density, as depicted in Fig. 6. In fact, when upstream demand is sufficiently high, a portion of it is directed to the dedicated lane, enabling the road to address a higher flow. The vehicles guided to the dedicated lane can keep moving there unless they have a public vehicle stopped in front. In such a condition, they are rerouted to the main road to avoid high densities in the dedicated lanes, causing a temporary increase in the main road density. In the conducted scenario, the sharing is slightly started once density of the first cell in the main road exceeds 48 veh/km, i.e. 70% of capacity, and reaches the maximum admissible lateral flow when the main road density reaches the critical value. When there is a planned stop in the ninth cell, vehicles start to leave the dedicated lanes from the previous cells and further redirection to the dedicated lanes is gradually getting cancelled, that avoids overly high densities in both dedicated and main spaces. It is evident that during the stop interval, the ninth cell remains unoccupied, and subsequently, vehicles are observed traversing this cell.

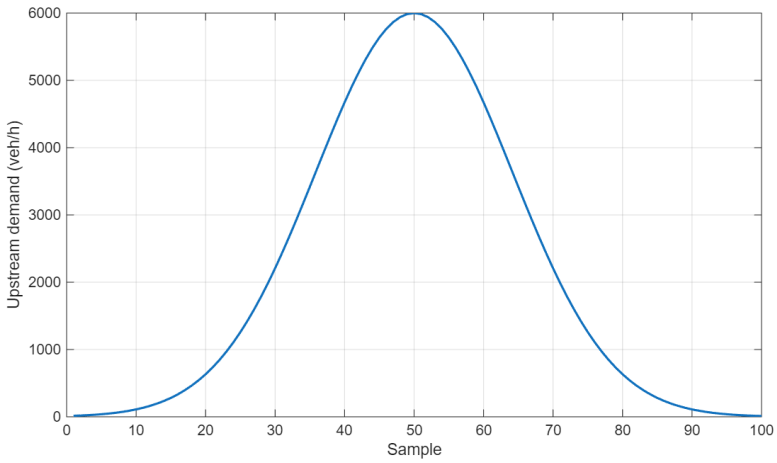


Figure 3: The upstream demand of the main road

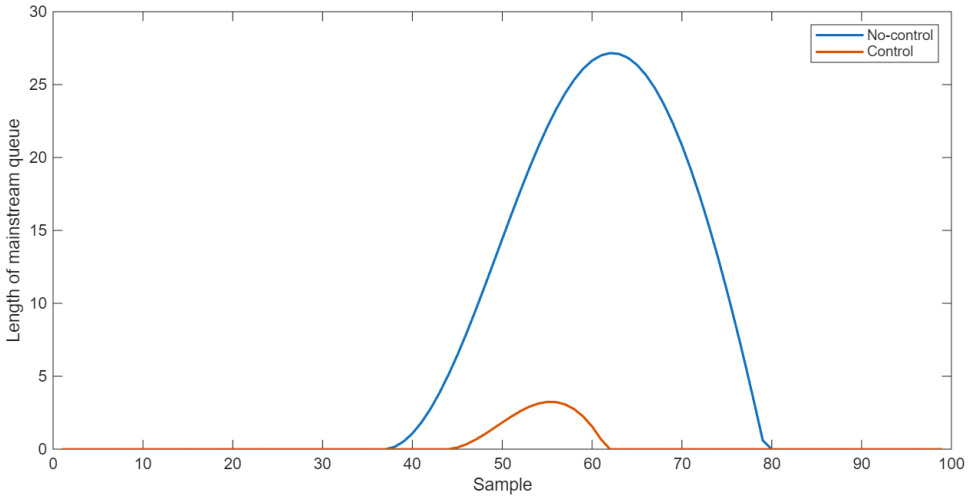


Figure 4: The length of queue upstream: The upstream queue length is notably decreased through the sharing strategy, resulting in a consequential decrease in the total travel time.

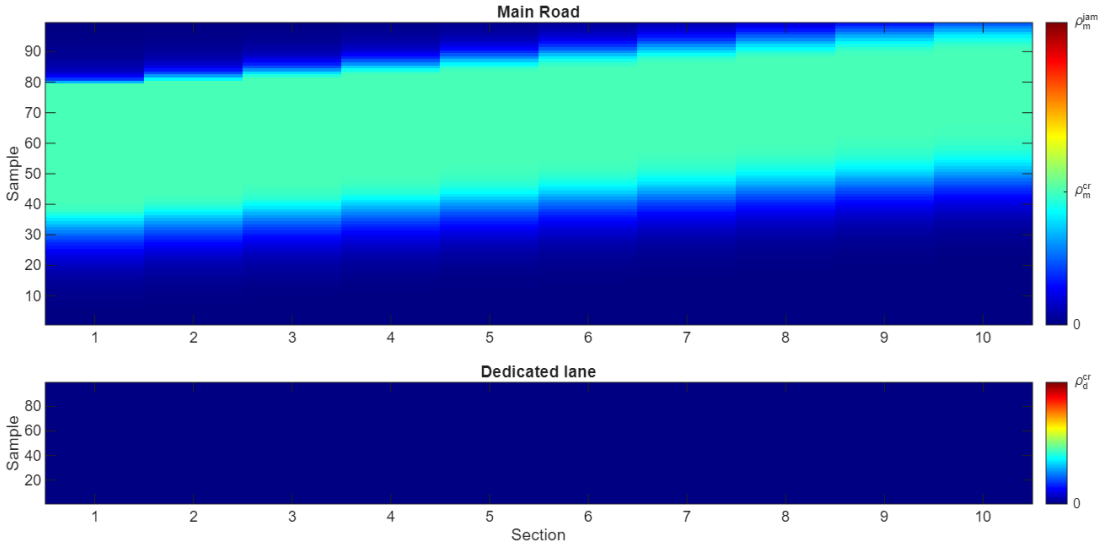


Figure 5: Road density in no-control case

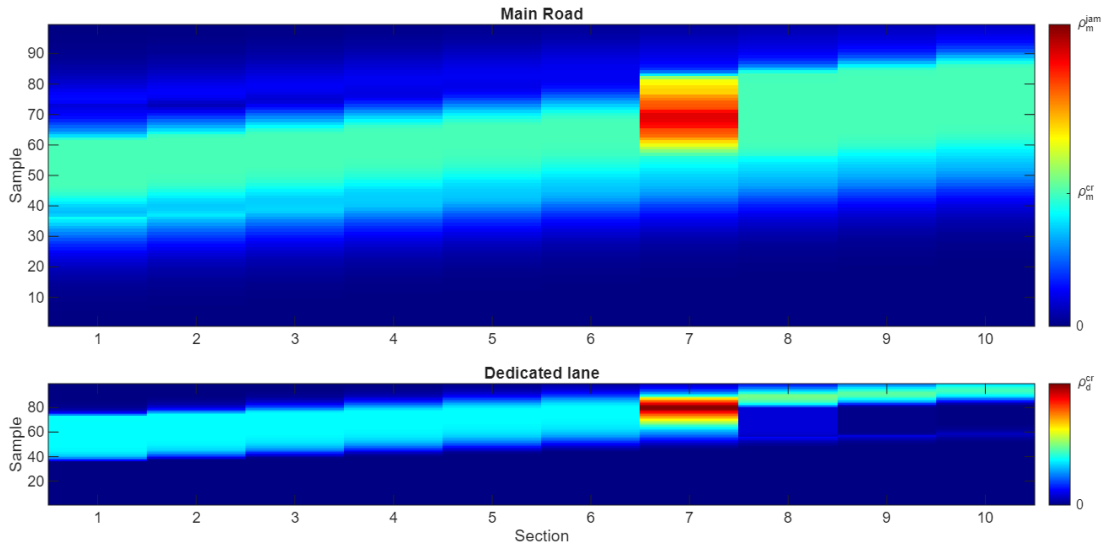


Figure 6: Road density in control case: Narrower green bands compared to Fig. 5 confirm that sharing the dedicated lane shortens the upstream queue. The planned stop made vehicles leave the dedicated lane, causing temporary increase in road density

5 Conclusions

The objective of this research was to develop a strategy for utilizing dedicated public transport lanes to improve traffic conditions, while ensuring that public transportation performance remains unimpaired. To this end, we established a macroscopic model to represent traffic dynamics and lateral flows between main road and the dedicated lanes. Following this, an optimal control problem was formulated to determine lateral flows, thereby minimizing a cost function aimed at mitigating congestion and also preventing unnecessary lateral movements. The CTM equations and appropriate limits on lateral flows, designed to maintain the dedicated lane in free-flow conditions, were incorporated as the OCP constraints. Finally, the OCP was solved via an iterative algorithm to obtain optimal lateral flows. Preliminary simulation results indicate the efficacy of the proposed method in improving traffic flow without compromising public transit performance.
The proposed method adopts a centralized strategy and relies on access to precise public transport information and measured aggregate traffic variables from both the main road and the dedicated lane, making it costly and computationally demanding for extensive infrastructure. Hence, future work could focus on enhancing its practicality through different measures such as decentralizing the OCP and accounting for uncertainties and missing data.

Acknowledgements

The work of the first author was supported by the MSCA COFUND CROP international postdoctoral program at Czech Technical University in Prague, Czechia, co-funded by the EU.

References

Ampountolas, K., Dos Santos, J. A., & Carlson, R. C. (2019). Motorway tidal flow lane control. *IEEE Transactions on Intelligent Transportation Systems*, *21*(4), 1687–1696.

Jiang, X., & Shang, Q. (2022). A dynamic cav-dedicated lane allocation method with the joint optimization of signal timing parameters and smooth trajectory in a mixed traffic environment. *IEEE Transactions on Intelligent Transportation Systems*, *24*(6), 6436–6449.

Keyvan-Ekbatani, M., Kouvelas, A., Papamichail, I., & Papageorgiou, M. (2012). Exploiting the fundamental diagram of urban networks for feedback-based gating. *Transportation Research Part B: Methodological*, *46*(10), 1393–1403.

Li, W., Li, J., & Han, D. (2023). Dynamic lane reversal strategy in intelligent transportation systems in smart cities. *Sensors*, *23*(17), 7402.

Liang, T., Bai, T., & Malikopoulos, A. A. (2026). Predictive lane-change and routing coordination in bus-priority mixed traffic corridors. *arXiv preprint arXiv:2603.01611*.

Luo, Q., Du, R., Jia, H., & Yang, L. (2022). Research on the deployment of joint dedicated lanes for cavs and buses. *Sustainability*, *14*(14), 8686.

Malekzadeh, M., Naderi, M., Jin, F., Bogenberger, K., Wang, Y., & Papageorgiou, M. (2025). A comprehensive review of tidal traffic flow control: From conventional lane reversal to emerging internal boundary control. *Results in Engineering*, 106198.

Malekzadeh, M., Papamichail, I., Papageorgiou, M., & Bogenberger, K. (2021). Optimal internal boundary control of lane-free automated vehicle traffic. *Transportation Research Part C: Emerging Technologies*, *126*, 103060.

Papageorgiou, M., Marinaki, M., Typaldos, P., & Makantasis, K. (2016). A feasible direction algorithm for the numerical solution of optimal control problems-extended version. *Chania, Greece: Technical University of Crete, Dynamics Sysyems and Simulations Laboratory*, *26*.

Roncoli, C., Papageorgiou, M., & Papamichail, I. (2015a). Traffic flow optimisation in presence of vehicle automation and communication systems–part i: A first-order multi-lane model for motorway traffic. *Transportation Research Part C: Emerging Technologies*, *57*, 241–259.

Roncoli, C., Papageorgiou, M., & Papamichail, I. (2015b). Traffic flow optimisation in presence of vehicle automation and communication systems–part ii: Optimal control for multi-lane motorways. *Transportation Research Part C: Emerging Technologies*, *57*, 260–275.

Shan, X., Wan, C., Hao, P., Wu, G., & Barth, M. J. (2024). Developing a novel dynamic bus lane control strategy with eco-driving under partially connected vehicle environment. *IEEE Transactions on Intelligent Transportation Systems*, *25*(6), 5919–5934.

Zhang, X., Bai, Q., Chen, L., & Cao, R. (2025). A review of dedicated lane deployment for connected and automated vehicles. *IEEE Transactions on Intelligent Transportation Systems*.